OPEN

Citation: Cell Death and Disease (2013) 4, e674; doi:10.1038/cddis.2013.188

www.nature.com/cddis

Eleostearic acid induces RIP1-mediated atypical apoptosis in a kinase-independent manner via ERK phosphorylation, ROS generation and mitochondrial dysfunction

S Obitsu[1], K Sakata[1], R Teshima[1] and K Kondo*[,1]

RIP1 is a serine/threonine kinase, which is involved in apoptosis and necroptosis. In apoptosis, caspase-8 and FADD have an important role. On the other hand, RIP3 is a key molecule in necroptosis. Recently, we reported that eleostearic acid (ESA) elicits caspase-3- and PARP-1-independent cell death, although ESA-treated cells mediate typical apoptotic morphology such as chromatin condensation, plasma membrane blebbing and apoptotic body formation. The activation of caspases, Bax and PARP-1, the cleavage of AIF and the phosphorylation of histone H2AX, all of which are characteristics of typical apoptosis, do not occur in ESA-treated cells. However, the underlying mechanism remains unclear. To clarify the signaling pathways in ESA-mediated apoptosis, we investigated the functions of RIP1, MEK, ERK, as well as AIF. Using an extensive study based on molecular biology, we identified the alternative role of RIP1 in ESA-mediated apoptosis. ESA mediates RIP1-dependent apoptosis in a kinase independent manner. ESA activates serine/threonine phosphatases such as calcineurin, which induces RIP1 dephosphorylation, thereby ERK pathway is activated. Consequently, localization of AIF and ERK in the nucleus, ROS generation and ATP reduction in mitochondria are induced to disrupt mitochondrial cristae, which leads to cell death. Necrostatin (Nec)-1 blocked MEK/ERK phosphorylation and ESA-mediated apoptosis. Nec-1 inactive form (Nec1i) also impaired ESA-mediated apoptosis. Nec1 blocked the interaction of MEK with ERK upon ESA stimulation. Together, these findings provide a new finding that ERK and kinase-independent RIP1 proteins are implicated in atypical ESA-mediated apoptosis.
Cell Death and Disease (2013) **4,** e674; doi:10.1038/cddis.2013.188; published online 20 June 2013
Subject Category: Neuroscience

Apoptosis has an important role in the normal development of multicellular eukaryotes and maintenance of adult organism homeostasis. Apoptotic cell death can be induced by two distinct pathways: intrinsic and extrinsic. In the extrinsic pathway, cell death begins with the binding of an appropriate ligand to death receptors, such as tumor necrosis factor (TNF) receptors on the cell surface, and then caspases are activated including caspase-8 and caspase-3.[1–3] However, caspases are not always involved in the cell death in the intrinsic pathway.[4] Programmed necrotic cell death or necroptosis, rather than accidental death (classic necrosis), has been characterized.[1,5–7] Necroptosis is a notable example of non-apoptotic cell death when cells are stimulated with TNF-α. Molecules that regulate necroptosis include receptor-interacting protein 1 (RIP1), RIP3, caspase inhibitors such as z-VAD-fmk and reactive oxygen species (ROS).[5,8–12] At least RIP3 is considered indispensable for necroptosis.[9,10,13] RIP3 regulates energy metabolism.[8] Both mixed lineage kinase domain-like protein (MLKL) and mitochondrial phosphatase PGAM5 function downstream of RIP3.[14,15] However, the underlying mechanisms still remain unclear. In contrast, RIP1 is involved in both apoptosis and necroptosis. In RIP1-dependent apoptosis, complex IIb, which includes RIP1, FADD and caspase-8, has a significant role in response to TNF stimulation or loss of IAP.[2,3,6,16] This complex activates caspase cascade to mediate apoptosis. Intermediate domain of RIP1 is required for activation of TNF-α receptor signaling event.[17] The domain determines switch between necroptosis and apoptosis. Like RIP3, the role of RIP1 in cell death remains to be defined. Specificity of necroptosis inhibitors has been reported.[18–20] Nec1 blocks both RIP1 and indoleamine-2,3-dioxygenase (IDO). Nec1 and Nec1i inhibited IDO. IDO inhibition appears not to be involved in cell death. Nec1i at higher concentrations inhibited necroptosis in mouse L929 cells, suggesting that Nec1i may target molecules other than RIP1. RIP1 is essential for TNF-α signaling to

[1]Division of Novel Foods and Immunochemistry, National Institute of Health Sciences, Tokyo, Japan
*Corresponding author: K Kondo, Division of Novel Foods and Immunochemistry, National Institute of Health Sciences, 1-18-1 Kamiyoga, Setagaya, Tokyo 158-8501, Japan. Tel: +81 3 3700 1141; Fax: +81 3 3707 6950; E-mail: kondo@nihs.go.jp
Keywords: apoptosis; AIF; RIP1; eleostearic acid; mitochondria; reactive oxygen species
Abbreviations: AIF, apoptosis-inducing factor; CCCP, carbonyl cyanide m-chrolophenyl hydrazine; COX, mitochondrial respiratory complex; Drp, dynamin-related protein; ERK, extracellular signal-regulated kinase; ESA, eleostearic acid; FADD, Fas-associated protein with death domain; GSH, glutathione; IDO, indoleamine-2,3-dioxygenase; MAPK, mitogen-activated protein kinase; MEK, MAPK/ERK kinase; Mn-SOD, manganese superoxide dismutase; NAC, N-acetyl cysteine; Nec, necrostatin; PARP, poly(ADP-ribose) polymerase; RIP, receptor-interacting protein; ROS, reactive oxygen species; TNF, tumor necrosis factor; TUNEL, Terminal deoxynucleotidyl transferase dUTP nick end labeling; Z-VAD-fmk, Z-Val-Ala-Asp-fluoromethylketone
Received 10.4.13; revised 30.4.13; accepted 30.4.13; Edited by M Agostini

mitogen-activated protein kinase (MAPK).[21] The mechanism by which RIP1 initiates MAPK activation is unclear. The kinase activity of RIP1 does not appear to be required for MAPK activation.[22,23] Mice lacking RIP1 causes postnatal death.[24] RIP1 is involved in both life and death. Interestingly, RIP3 expression in human and mouse brain tissues was reported to be low.[25,26]

We previously found that α-eleostearic acids (ESA), a conjugated tri-enoic fatty acid, obtained by *in vitro* screening from *Pleurocybella porrigens* mushrooms, exert a novel type of programmed cell death, which is AIF-dependent.[27] Since then, we have been interested in this fatty acid because the ingestion of *P. porrigens* mushrooms led to an outbreak of convulsive encephalopathy in patients with a history of chronic renal failure, resulting in 19 deaths in Japan. Death rates reached up to 32%. A cytotoxic fatty acid ($IC_{50} = 46.5\ \mu$g/ml in B16F1 cells) and unusual amino acids (toxicity in glial cells at several tens of μg/ml) have been isolated from these mushrooms by other groups.[28–30] Although, many researchers tried to find a causative substance related to the encephalopathy, no evidence has been found so far. In addition, ESA-mediated apoptosis appears to be a novel type of ERK1/2- and RIP1-dependent cell death. We isolated several fatty acids that exert cell cytotoxicity as well as ESA.[31,32] The relationship between cytotoxic fatty acids and acute encephalopathy caused by ESA remains to be solved. As previously reported,[27] as low as 2 μg/ml ESA induces atypical apoptotic cell death, which is blocked by α-tocopherol (Toc), the MEK inhibitor U0126 and MEK1/2 knockdown. ESA induces caspase- and poly(ADP-ribose) polymerase-1 (PARP-1)-independent cell death associated with the membrane blebbing, cell shrinkage, translocation of AIF and the formation of apoptotic bodies. ESA appears to activate a novel cell death pathway. However, the underlying mechanisms remain to be solved. In this study, we investigated ROS generation, the phosphorylation status of AIF, RIP1 and ERK1/2, and the effect of RIP1 inhibitors such as necrostatin-1 (Nec1), Nec1 inactive control (Nec1i) and Nec5 on ESA-mediated apoptosis. The generation of ROS in mitochondria, the mitochondrial membrane potential, the intracellular level of GSH, and the effect of several antioxidants on ESA-mediated apoptosis were also investigated to clarify the mechanisms.

Here, we show that a novel RIP1-dependent apoptotic cell death induced by ESA is mediated through MEK/ERK pathway. ESA-mediated apoptosis is associated with the decrease in phosphorylation of AIF and RIP1, the nuclear translocation of AIF and ERK1/2, and ROS production. ROS generation in mitochondria results in the disruption of mitochondrial cristae structure, leading to cell death.

Results

AIF/RIP1-dependent but RIP3-independent cell death is induced by ESA. ESA elicited apoptotic cell death as shown by membrane blebbing and apoptotic body formation, chromatin condensation, and cell shrinkage in neuronal PC12, SH-SY5Y and NG108-15 cells, as well as rat primary neurons and FBD-102b oligodendrocytes (Figure 1a). As reported, ESA-mediated apoptosis is neither caspase-3-dependent nor PARP-1-dependent.[27] Bax is not translocated to mitochondria upon ESA stimulation. ESA-mediated apoptosis is AIF-dependent, which is translocated to the nucleus upon ESA stimulation. However, the underlying mechanisms remain unclear. To better understand the mechanisms, the effect of antioxidants, anti-apoptotic Bcl-2 proteins, Bcl-2 and Bcl-X_L on ESA-mediated apoptosis was examined. Rat cortical neurons cultured in B27-supplemented media survived, whereas the cells in the media lacking Toc and other antioxidants (B27-AO) were killed by ESA. Dendrites were disrupted in ESA-treated cells. This indicates that antioxidants are effective in preventing ESA-mediated apoptosis (Figure 1b). Either Bcl-2 or Bcl-X_L, or the combination of both proteins had no inhibitory effect on ESA-mediated apoptosis. In contrast, knockdown of AIF and RIP1 blocked ESA-mediated apoptosis. RIP1 as well as AIF has an important role in ESA-mediated apoptosis. Synergistic effect of siRNAs between AIF and RIP1 against ESA-mediated apoptosis was not observed, suggesting that AIF and RIP1 function in the same pathway (Figure 1c). RIP3 knockdown did not show any protective effect, indicating that RIP3 is not involved in ESA-mediated apoptosis. Immunoblotting data revealed that a significant amount of RIP3 was not expressed in PC12 cells. RIP3 might not be important in neuronal cells. The necroptosis inhibitor necrostatin-1 (Nec1) and its inactive control (Nec1i) blocked ESA-mediated apoptosis, whereas Nec5 had no effect (Figure 1d).

ESA mediates ROS generation in mitochondria, which is scavenged by antioxidants. ROS was generated in PC12 and FBD-102b cells when these cells were stimulated with ESA for several hours. To estimate the amount of ROS generated by ESA, we used two fluorescent probes, MitoSOX for detecting mitochondrial superoxides, and BESSo for intracellular superoxides. ESA triggered a small amount of ROS production in mitochondria and intracellular space (Figure 2a, left panel). The amount was much lower than that in activated macrophage. We could detect a small amount of ROS generation because the basal ROS generation in PC12 cells was extremely low. A larger amount of ROS was produced in FBD-102b oligodendrocytes several hours after ESA stimulation as compared with PC12 (Figure 2a, right panel). Toc and its derivative tocotrienol effectively suppressed both ROS generation (Supplementary Figure 1) and ESA-mediated apoptosis at a physiological concentration ($< 0.2\ \mu$g/ml) (Figure 2b). Acetylated form of Toc (Toc-Ac) did not effectively block ESA-mediated apoptosis. The apoptosis was also inhibited by antioxidants, such as quercetin, EGCG, sesaminol and NAC at higher concentrations (Figure 2c). Grape seed procyanidins (GSP, polymerized catechins), which are not membrane-permeable due to numerous hydroxyl groups and its molecular size, had no effect on protecting ESA-mediated apoptosis. These results suggest that phenolic hydroxyl groups in hydrophobic inhibitors were essential for preventing ESA-mediated apoptosis. The MEK inhibitor U0126 also reduced ESA-triggered ROS generation (Figure 2a). This suggests that U0126 is upstream of ROS generation.

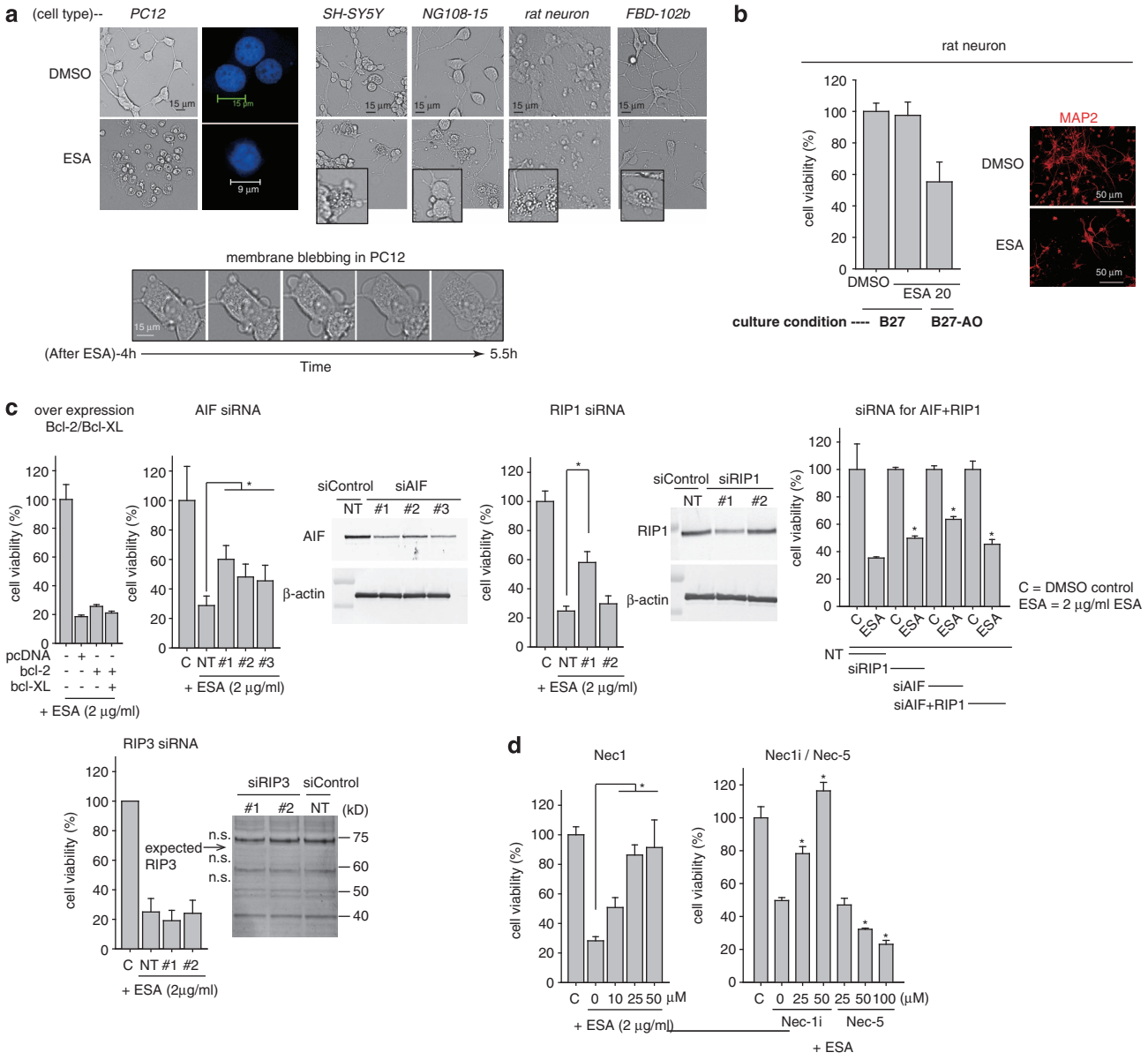

Figure 1 ESA induces apoptotic cell death in neuronal cells. (**a**) PC12, SH-SY5Y, NG108-15 and FBD-102b cells, as well as rat cortical neurons were used to observe morphological changes of ESA-mediated apoptosis. Cells were cultured under a differentiation condition (in the case of cell lines) and exposed to 2 μg/ml ESA for several hours in cell lines and 48 h in rat neurons. ESA initiated membrane blebbing and formation of apoptotic bodies in neuronal cells (*inset* in each figure). The time course of morphological changes in PC12 cells is shown at the bottom, indicating clear membrane blebbing at 4 h after ESA treatment. Nucleus of PC12 cells treated with DMSO or ESA were shown in blue (Hoechst 33342 staining). (**b**) Rat neurons cultured in B27-supplemented media survived, whereas the cells in antioxidant-deficient B27-AO-supplemented media were killed by ESA (20 μg/ml) for 48 h. Values are the means ± S.D. ($n = 3$; $^*P < 0.05$ to DMSO control). Dendrites of rat neurons were stained with anti-MAP2 antibody (red). ESA disrupted the dendrites. (**c**) ESA-mediated apoptosis is AIF/RIP1-dependent and RIP3-independent in neuronal cells. Cells transfected with pcDNA, pcDNA-bcl-2, or pcDNA-bcl-X_L were exposed to ESA. Bcl-2 and Bcl-X_L did not block ESA-mediated apoptosis. Knockdown of AIF and RIP1 blocked ESA-mediated apoptosis. Double knockdown (AIF/RIP1) had no synergistic effect against ESA-mediated apoptosis. Cell viability of RIP3-knockdown cells is the same as non-target control (NT) when stimulated with ESA. RIP3 protein was hardly expressed in PC12 cells. Western blot data of cells knocked down with AIF, RIP1, and RIP3 were shown. NT, non-target control in siRNA experiments. (**d**) Nec1 blocked ES-mediated apoptosis, whereas Nec5 did not. Nec1 inactive control, which cannot block necroptosis, inhibited ESA-mediated apoptosis.

Next, we examined ATP production, the mitochondrial membrane potential, intracellular levels of glutathione (GSH) in ESA-treated cells with or without inhibitors. ATP was decreased in ESA-treated cells in a dose-dependent manner, which was rescued by Nec1, U0126 and Toc (Figure 2d). The ATP reduction occurred 4 h after ESA stimulation, indicating time dependency. The mitochondrial membrane potential was decreased immediately and slightly increased 4 h after ESA stimulation (Figure 2e). However, the potential did not disappear until the final stage of cell death. Intracellular GSH levels were not decreased in ESA-treated cells. An inhibitor of GSH synthesis, BSO (10 μM) dramatically

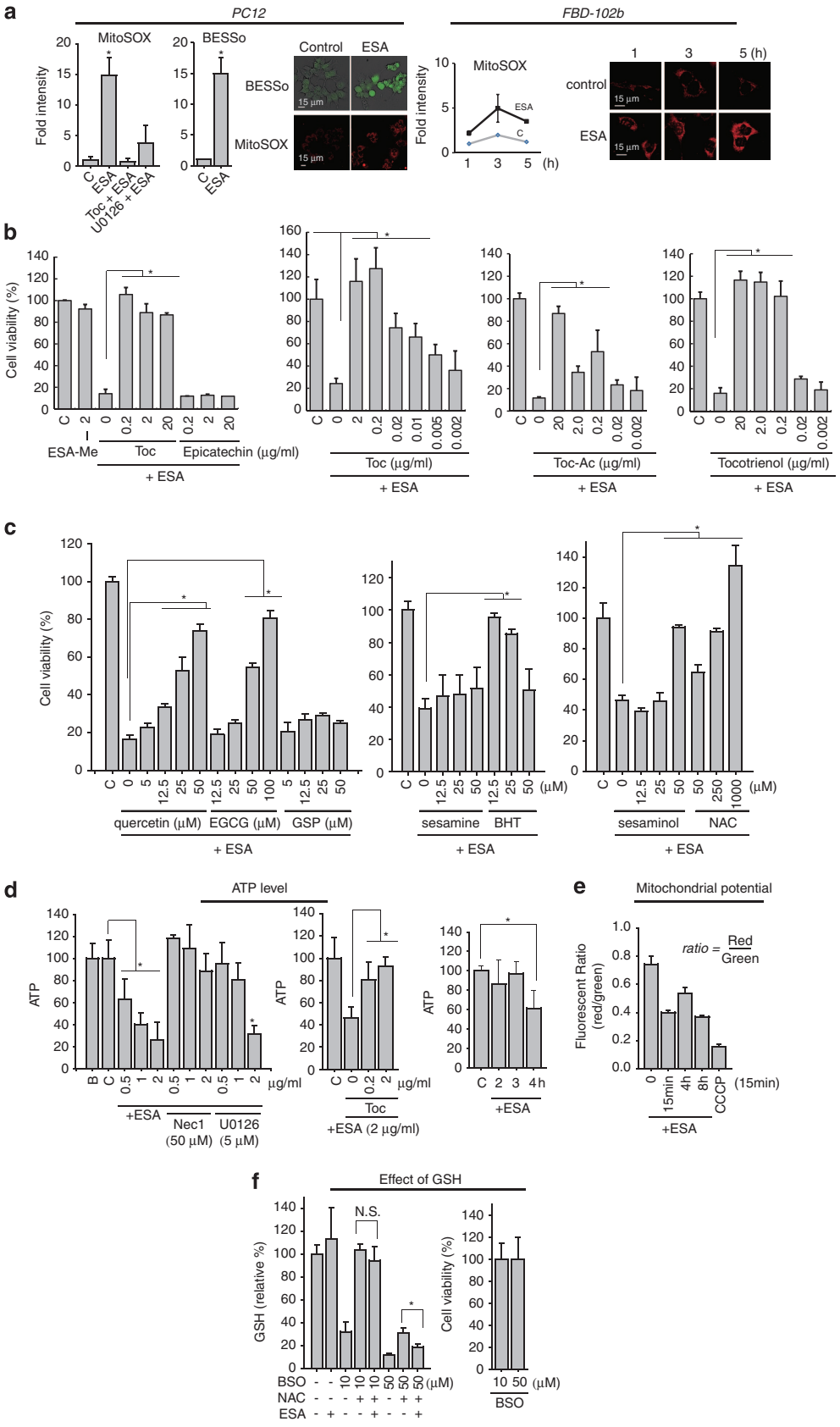
a
PC12
FBD-102b
MitoSOX
BESSo
Control
ESA
Fold intensity
C
ESA
Toc + ESA
U0126 + ESA
BESSo
MitoSOX
15 μm
1
3
5 (h)
control
b
Cell viability (%)
ESA-Me
Toc
Epicatechin (μg/ml)
+ ESA
Toc (μg/ml)
Toc-Ac (μg/ml)
Tocotrienol (μg/ml)
c
quercetin (μM)
EGCG (μM)
GSP (μM)
sesamine
BHT
sesaminol
NAC
(μM)
d
ATP level
ATP
μg/ml
+ESA
Nec1 (50 μM)
U0126 (5 μM)
Toc
+ESA (2 μg/ml)
e
Mitochondrial potential
Fluorescent Ratio (red/green)
ratio = Red / Green
15min
4h
8h
CCCP
f
Effect of GSH
GSH (relative %)
N.S.
BSO
NAC
ESA
Cell viability (%)

reduced the intracellular GSH level, which was rescued by *N*-acetyl cysteine (NAC, 1 mM). BSO (50 μM) completely depleted GSH, which recovered in part by NAC (1 mM). However, GSH depletion itself did not trigger cell death (Figure 2f). NAC blocked ESA-mediated apoptosis. Therefore, an additional increase in GSH by NAC may contribute to block ESA-mediated apoptosis. Alternatively, the increase in the redox potential in mitochondria may be important.

Nuclear localization of both AIF and ERK is necessary for ESA-mediated apoptosis. As we reported,[27] AIF has an important role in ESA-mediated apoptosis. Confocal microscopic studies revealed that DNA cleavage occurred near AIF proteins (Figure 3a). Illustration shows that TUNEL staining (red) overlapped with AIF staining (green). The nuclear localization of AIF was seen in FBD-102b cells and rat neurons (Figure 3b). ESA induced the partial cleavage and the release of AIF into cytosolic fraction mainly as a full-length form. In addition, mitochondrial matrix proteins, complex Vα-subunit (COX Vα) and manganese superoxide dismutase (Mn-SOD) were also released to the cytoplasm upon ESA stimulation (Figure 3c). Next we investigated whether AIF itself triggered ESA-mediated apoptosis. Deletion mutant ΔN102-AIF tagged with GFP (ΔN102-AIF–GFP), which lacks 102 amino acids at the *N*-terminus of AIF, was constructed to be expressed in the nucleus without stimulation. ΔN102-AIF–GFP did not induce cell death although the AIF was localized in the nucleus (Figure 3d). Cyclophilin A (cyp-A) was reported to participate in AIF translocation to the nucleus.[33] Therefore, the involvement of cyp-A was investigated in ESA-mediated apoptosis. Knockdown of cyp-A did not block ESA-mediated apoptosis despite the colocalization of AIF and cyp-A in the nucleus (Figure 3e). AIF is reported to have an important role in programmed necrosis by interacting with histone H2AX.[4] Since we reported that histone H2AX was not phosphorylated upon ESA stimulation, we examined another molecule other than cyp-A and histone H2AX. The complete inhibition of ESA-mediated apoptosis by U0126 suggests the importance of the MEK/ERK signaling pathway.[27] We examined whether ERK activation is required for AIF-dependent cell death by ESA. An agonist of MEK/ERK pathway, 4-hydroxytamoxifen (4-HT) failed to induce cell death in ΔN102-AIF-transfected cells. Thus, to localize ERK in the nucleus together with AIF, PC12 cells were treated with leptomycin B (Lep-B). The viability of cells transfected with ΔN102-AIF was significantly decreased as compared with that of cells transfected with GFP when transfection was performed by the lipofection method. A similar result was obtained from the electroporation method, which was not significant but has a strong tendency (Figure 3f). Although colocalization of AIF with ERK1/2 was in part in the nucleus, the presence of the two proteins in the nucleus may be important for ESA-mediated apoptosis.

Mitochondrial fission can affect apoptosis. To investigate whether ablation of mitochondrial fission inhibited or suppressed ESA-mediated apoptosis, dynamin-related protein-1 (Drp1, also known as Dnm1 or Dlp1) was knocked down by siRNA in PC12 and SH-SY5Y cells. Knockdown of rat Drp1 caused the formation of fused mitochondria (Supplementary Figure 2a). However, ESA-mediated apoptosis was not inhibited by Drp1 knockdown, which was distributed largely in the cytosol of resting cells and appeared functional. Moreover, Drp1 knockdown in SH-SY5Y cells had no effect. In addition, an inhibitor of mitochondrial fission, Mdivi-1, did not affect cell viability (Supplementary Figures 2b and c), suggesting that signaling pathways upstream of mitochondrial fission are important in ESA-mediated apoptosis.

RIP3 is not involved in ESA-mediated apoptosis. RIP3 as well as RIP1 is involved in TNF receptor-induced necroptosis.[8–10] At least RIP3 is essential for necroptosis.[13] Ubiquitination of RIP1 followed by its deubiquitination was initiated, and led to necroptosis upon TNF receptor stimulation in the presence of Z-VAD-fmk.[1] RIP1 ubiquitination was observed when PC12 cells were treated with TNF-α along with Z-VAD-fmk (Figure 4a). On the other hand, ESA stimulation alone did not initiate RIP1 ubiquitination even in the presence of Z-VAD-fmk (Figures 4b and c), suggesting no involvement of TNF-α receptor. In caspase-8-deficient SH-SY5Y cells, apoptosis was induced by ESA. This is consistent with this result. Next, we examined the involvement of RIP3 in ESA-mediated apoptosis. When Balb/c 3T3 cells were treated with TNF-α along with Z-VAD-fmk, RIP3 was associated with RIP1. Nec1 blocked the association and degradation of RIP1 and RIP3. However, RIP3 was not associated with RIP1 when PC 12 cells were treated with ESA with or without Z-VAD-fmk (Figures 4c and d). These results indicate that ESA did not induce RIP3 activation.

Figure 2 ESA triggers ROS generation in mitochondria, which is blocked by antioxidants. (**a**) Mitochondrial ROS and intracellular ROS were measured using fluorescent probes, MitoSOX and BeSSo-AM, respectively. Images in PC12 cells were obtained from ESA-treated cells for 5 h, and the fluorescent intensity of each image (three fields per sample were obtained) was quantified using the MetaMorph software. ROS was generated in mitochondria, which was suppressed by Toc (2 μg/ml) and U0126 (5 μM). In FBD-102b cells, the time course of fluorescent intensity was investigated. Data were obtained from two independent experiments. (**b**) Toc and tocotrienol blocked ESA (2 μg/ml) apoptosis at a concentration of 0.2 μg/ml or below, whereas 20 μg/ml Toc-Ac was needed to prevent ESA-mediated apoptosis. Methyl ester of ESA (ESA-Me) did not induce cell death. (**c**) Antioxidants blocked ESA-mediated apoptosis. BHT, EGCG, GSP, Quercetin, sesamine, sesaminol and NAC were tested. BHT blocked ESA-mediated apoptosis at a physiological concentration (12.5 μM). For other antioxidants, higher concentrations were needed to prevent ESA-mediated apoptosis (50 μM). Data were obtained from at least two independent experiments in triplicates. Values are the means ± S.D. ($n = 6, 9$; $^*P < 0.05$ to ESA-treated cells). (**d**) ATP level was decreased in a dose-dependent manner upon ESA (2 μg/ml) stimulation. Nec1 (50 μM), U0126 (5 μM) and Toc (2 μg/ml) recovered the decrease in ATP level in ESA-treated cells. ATP levels were measured 5 h after ESA stimulation (*left and middle panels*). ATP depletion was time-dependent, and the reduction in ATP occurred 4 h after ESA stimulation (*right panel*). (**e**) Mitochondrial membrane potential was decreased to 50% as compared with control (time = 0 min) upon ESA stimulation. The potential did not disappear until the final stage of cell death. CCCP (50 μM) disappeared the potential. (**f**) Intracellular GSH levels were measured when cells were treated with or without BSO (10 or 50 μM) and NAC (1 mM). PC12 cells were cultured in the presence of BSO for 48 h, and then ESA (2 μg/ml) was added to the cells pretreated with buffer or NAC. Cell viability and GSH levels were measured 4 h after ESA addition. ESA did not affect intracellular GSH levels. Decrease in GSH by BSO did not trigger cell death. Values are the means ± S.D. $^*P < 0.05$ ($n = 3$, 6 in **d**, **f**).

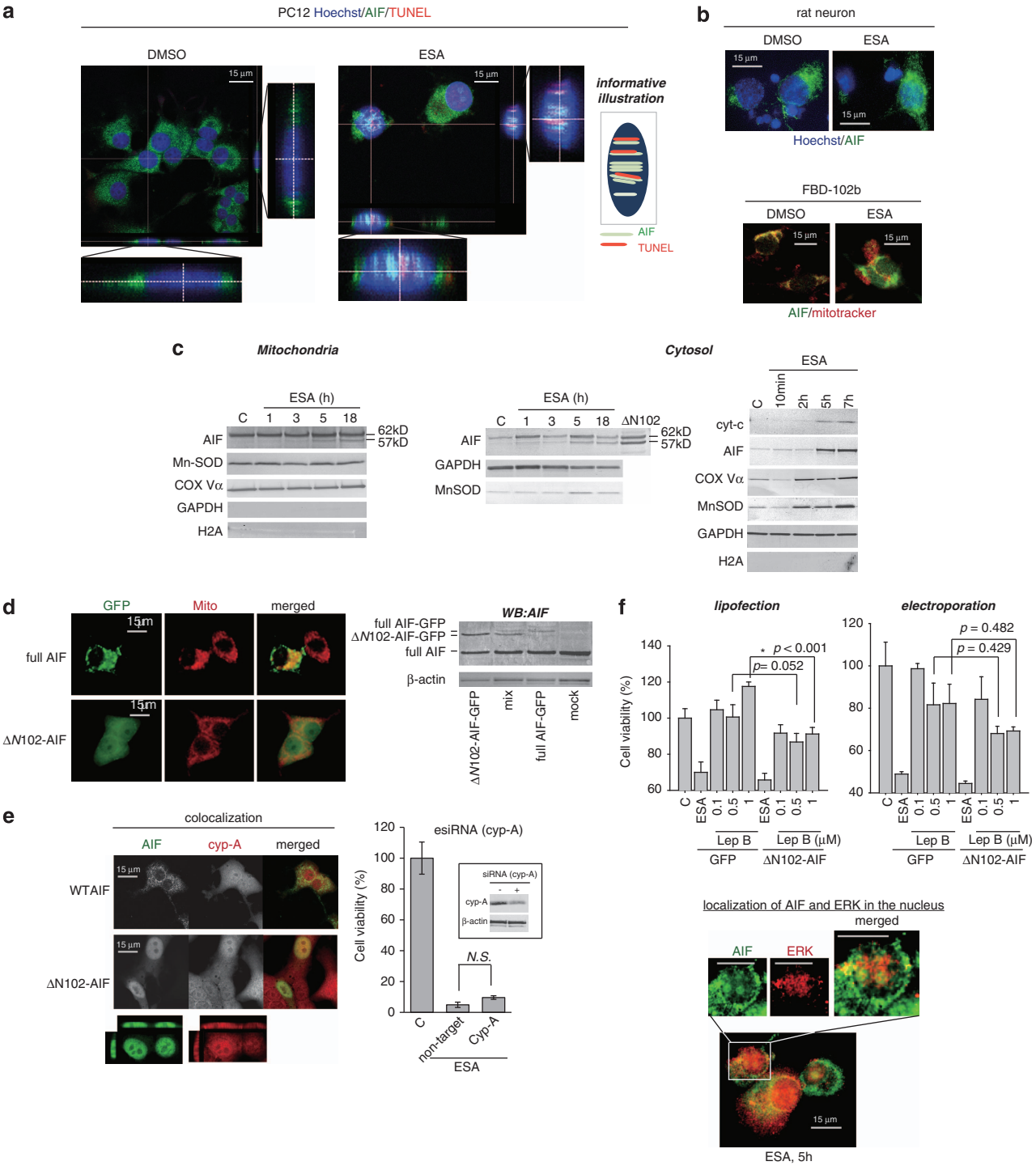

Figure 3 AIF translocation to the nucleus triggers ESA-mediated apoptosis together with ERK. (**a**) AIF was localized in the nucleus in PC12 cells 5 h after ESA stimulation as shown in 3D images. AIF, nuclei and DNA cleavage by TUNEL were labeled in green, blue and red, respectively. Informative illustration shows that TUNEL staining overlapped with AIF. (**b**) AIF translocation was observed in FBD-102b cells and rat cortical neurons. Images were obtained from cells treated with ESA for 5 h (FBD-102b) or 48 h (rat neurons). (**c**) Subcellular fractionation experiments show the release of AIF, COX Vα and Mn-SOD into the cytoplasm. (**d**) Deletion mutant ΔN102-AIF, which lacks 102 amino acids at the *N*-terminus, did not induce cell death by itself, although it was expressed in the nucleus. (**e**) Cyp-A is not necessary for ESA-mediated apoptosis. ΔN102-AIF-GFP did not initiate cell death, despite colocalization of AIF and endogenous Cyp-A in the nucleus. siRNA for Cyp-A was not able to suppress ESA-mediated apoptosis in PC12 cells. Values are the means ± S.D. ($n = 3$). NS represents not significant. (**f**) Lep-B, which is forced to induce the nuclear localization of ERK1/2, exacerbated cell viability only in ΔN102-AIF-transfected cells. Partial colocalization of both AIF and ERK1/2 was seen ESA-treated cells. The presence of AIF and ERK1/2 in the nucleus appears to be necessary for ESA-mediated apoptosis. Experiments were performed in two transfection conditions, lipofection and electroporation. Cell viability data were obtained from two independent experiments in triplicates.

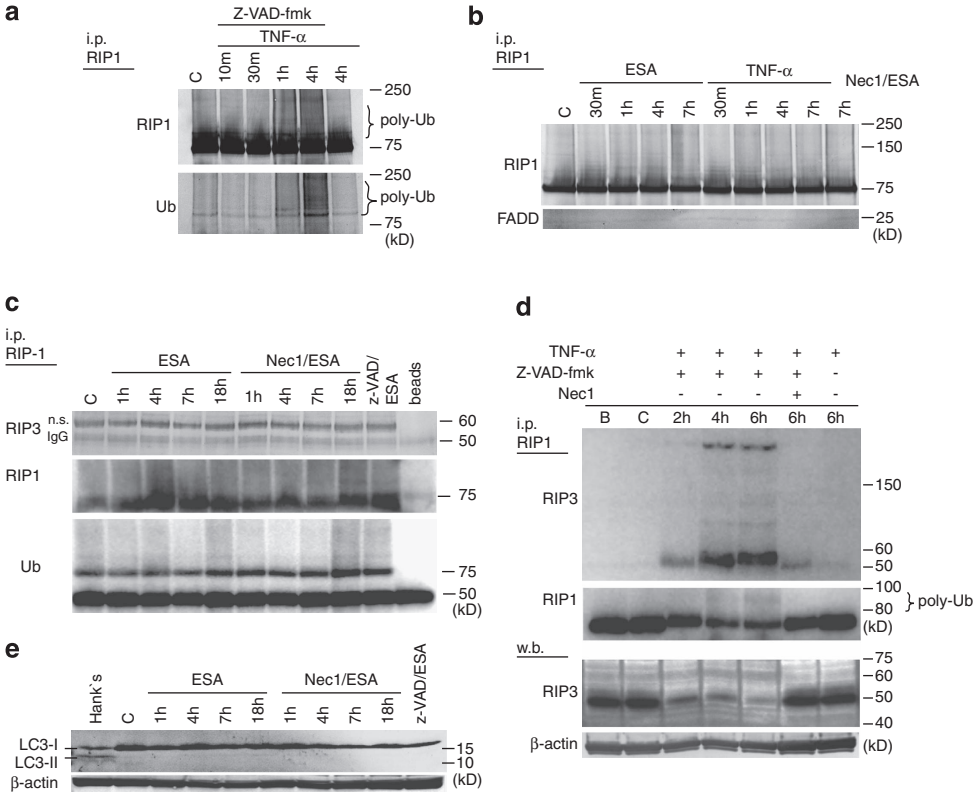

Figure 4 RIP3 is not involved in ESA-mediated apoptosis. (**a**) RIP1 was ubiquitinated by TNF-α (100 ng/ml) along with Z-VAD-fmk (20 μM) in PC12 cells. TNF-α alone did not undergo ubiquitination. (**b**) RIP1 uniquitination was not observed after ESA (2 μg/ml) stimulation. (**c**) RIP1 was not ubiquitinated by ESA in the presence of Nec1 (50 μM) and Z-VAD-fmk (20 μM). (**d**) RIP3 was expressed in 3T3 fibroblasts, and associated with RIP1 when the cells were treated with both TNF-α (25 ng/ml) along with z-VAD-fmk (50 μM). Association of RIP3 with RIP1 occurred a few hours after stimulation. At the same time, both RIP proteins were degraded. Nec1 (36 μM) inhibited association of RIP1 with RIP3. TNF-α alone did not induce the interaction. (**e**) Involvement of autophagy was examined. LC3-II derived from autophagosomes was not observed in cells treated with ESA (2 μg/ml) alone or with z-VAD-fmk (20 μM). Cells cultured in Hank's buffer for 1 h produced the autophagic LC3-II band, which was used as a positive control.

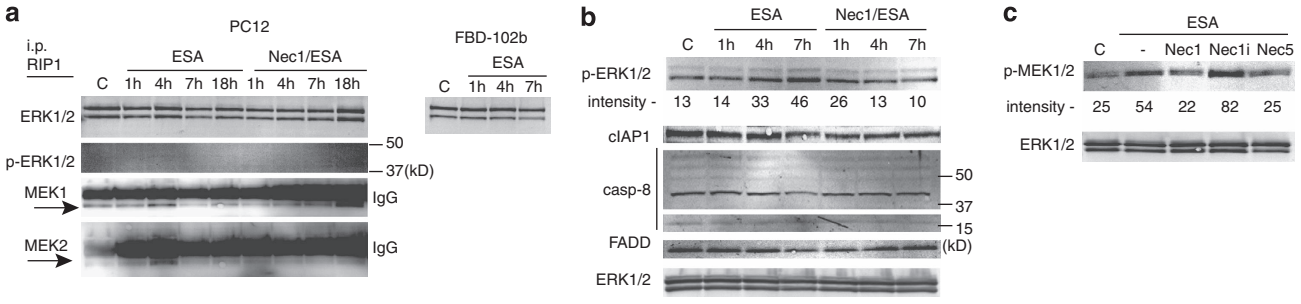

Figure 5 ERK1/2 is activated through MEK1/2 phosphorylation and association with RIP1 complex. (**a**) Phosphorylation of ERK1/2 was triggered by ESA, but was impaired by Nec1. (**b**) ERK1/2 was constitutively associated with RIP1 regardless of ESA stimulation. MEK1/2 formed the complex containing RIP1 and ERK1/2 to phosphorylate ERK1/2. (**c**) ESA induced MEK1/2 phosphorylation, which was suppressed by Nec1 and Nec5, but not Nec1i.

Caspase-8 and FADD were not associated with RIP1 (Figures 4b and 5b). Involvement of autophagy was next examined. ESA did not induce LC3-II formation, indicating that autophagy is not involved in ESA-mediated apoptosis (Figure 4e).

Phosphorylation of ERK1/2 occurred upon ESA stimulation.[27] To better understand the role of MEK/ERK pathway, immunoprecipitaion experiments (ip) were performed using mouse monoclonal RIP1 antibody (IgG2a). ERK1/2 proteins were constitutively associated with RIP1 regardless of ESA stimulation in PC12 and FBD-102b cells. In contrast, ERK1/2 was phosphorylated by ESA. MEK2, one of the MAPKKs, was also associated with RIP1 and phosphorylated in response to ESA. However, phosphorylated ERK1/2 was not seen on the blot of RIP1-immunoprecipitated samples. Active forms of caspase-8 were not produced by ESA (Figures 5a and b). Inhibitors of RIP1 activity, Nec1 and Nec5, but not Nec1i (inactive form of Nec1), impaired MEK1/2 phosphorylation

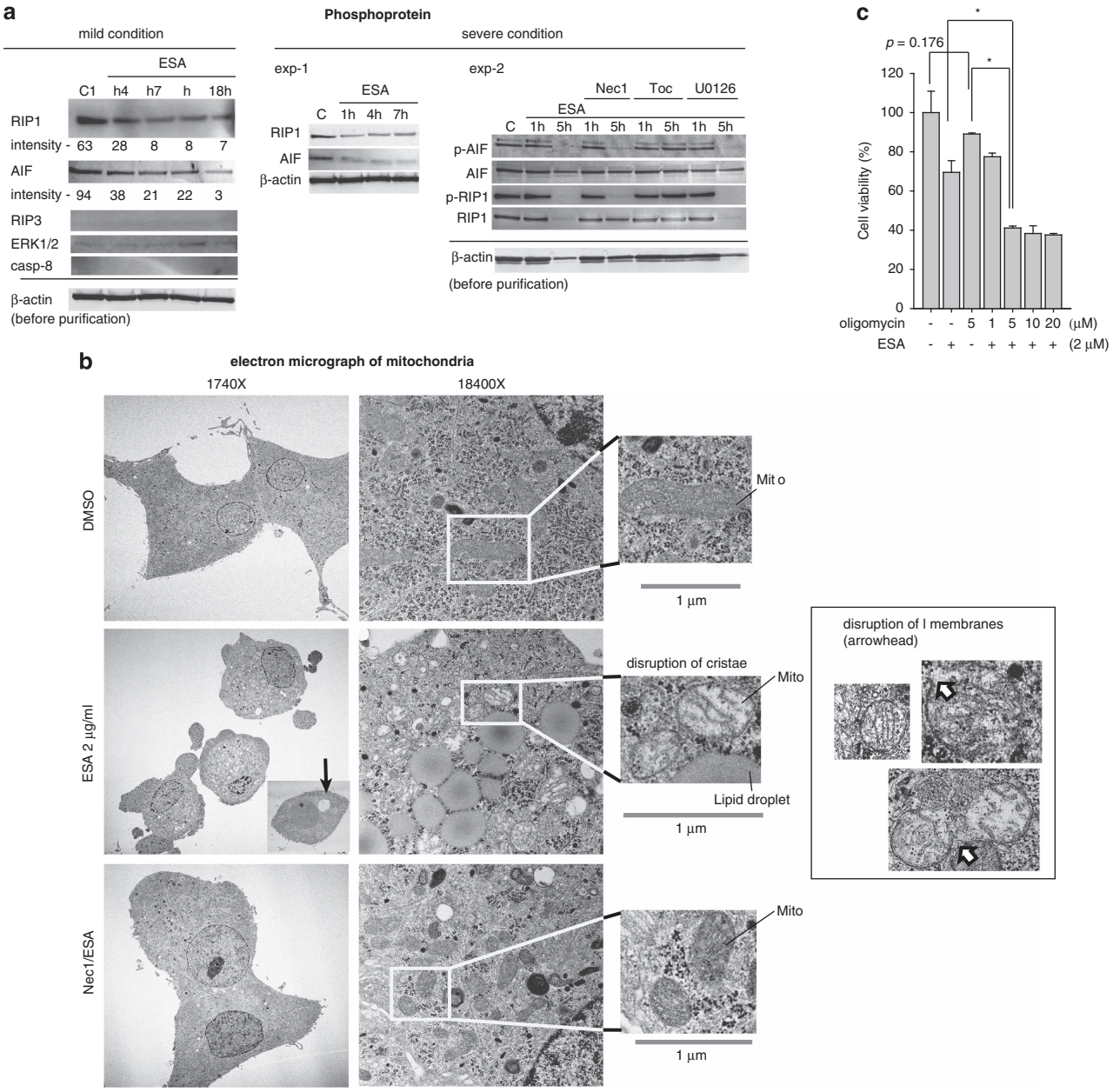

Figure 6 AIF and RIP1 are dephosphorylated by ESA. (**a**) PC12 cells were stimulated with ESA at two different concentrations, mild and severe (2 and 3.3 μM in 10-cm dish, respectively). ESA gradually initiated dephosphorylation of both AIF and RIP1 in a time-dependent manner in the mild condition. In the severe condition, the dephosphorylation occurred rapidly (exp-1). Dephosphorylation of AIF was occurred by 5 h after ESA stimulation (exp-2). Unlike AIF, RIP1 protein was not collected due to disruption of the membrane integrity (exp-2). Toc blocked RIP1 dephosphorylation. (**b**) Transmission electron microscopic analysis shows formation of apoptotic bodies and disruption of mitochondrial cristae. The long flat mitochondrial cristae structure was destroyed by ESA. Mitochondrial inner and outer membranes of some mitochondria in ESA-treated cells were collapsed. Nec1 prevented the mitochondrial damage. (**c**) Effects of oligomycin on ESA-mediated apoptosis. Oligomycin had a synergistic effect on ESA-mediated apoptosis. Data were obtained from two independent experiments in triplicates. Values are the means ± S.D. $^*P<0.05$ ($n=6$).

(Figure 5c). Taken together, ESA activates ERK pathway through MEK2, which is blocked by U0126 and Nec1. RIP1 may be involved in ERK pathway.

Decrease in AIF/RIP1 phosphorylation has an important role in ESA-mediated apoptosis. To investigate whether ESA induces RIP1 phosphorylation, we used a phosphorylated protein purification column because there is no antibody against phosphorylated RIP1. The concentration of total proteins in each cell lysate was adjusted to the same between the samples before the lysate was applied onto the column, and was confirmed by westernblotting using a β-actin antibody. We performed the study in two conditions, mild and severe. Surprisingly, in a mild condition (ESA 2 μg/ml in 10-cm dish), AIF and RIP1 were gradually dephosphorylated over several hours (Figure 6a, left panel). Phosphorylated RIP3 was not observed. In a severe condition, (ESA 3.3 μg/ml in 10-cm dish), both AIF and RIP1 were immediately dephosphorylated (Figure 6a, left panel, experiment 1). In experiment 2, some cells were

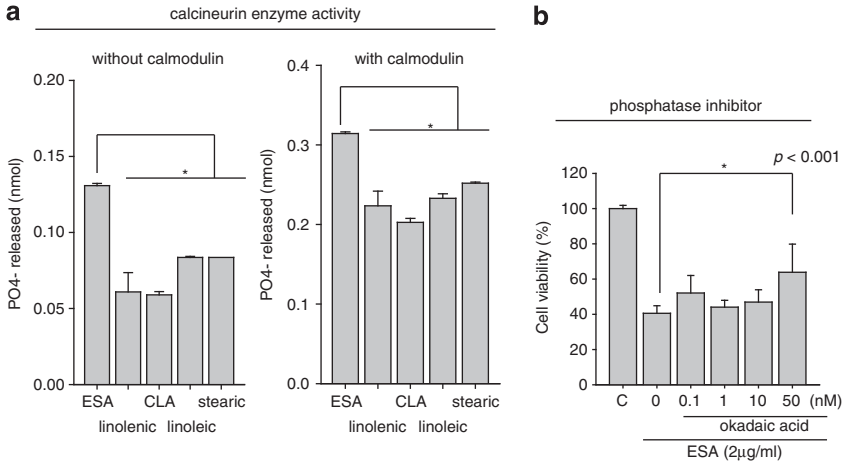

Figure 7 ESA activates Ser/Thr phosphatase calcineurin. (**a**) Enzymatic activity of calcineurin was measured with or without calmodulin. ESA augmented calcineurin activity regardless of calmodulin. (**b**) Okadaic acid, a phosphatase inhibitor, significantly reduced ESA-mediated apoptosis. Data were obtained from two independent experiments in triplicates. Values are the means ± S.D. $^*P<0.05$ ($n=6$).

severely damaged, and the cytosolic contents were released into culture media due to the disruption of plasma membrane integrity. Thus, RIP1 protein was hardly collected from cell lysates after 5-h ESA treatment. However, mitochondrial AIF protein was detected, and the collected AIF was not phosphorylated. Even in the severe condition, Toc blocked the AIF dephosphorylation. On the other hand, Nec1 and U0126 did not block AIF dephosphorylation.

Using transmission electron microscope, we next investigated the structure of mitochondria in PC12 cells treated with ESA (Figure 6b). Mitochondria in resting cells were 1 mm long and have normal cristae structure. In ESA-treated cells, the cristae were severely damaged, and disruptions of mitochondrial inner and outer membranes were observed. This is consistent with our result demonstrating the release of Mn-SOD and COX Vα into the cytoplasm. Mitochondrial disruption was blocked by Nec1. These results suggest that ESA may influence finally on the mitochondrial respiratory chain. Lipid droplets (LDs) were observed in ESA-treated cells, whereas formation of LDs was blocked by Nec1. To further examine the effect of ESA on mitochondrial electron transport system, its inhibitor was tested together with ESA. Oligomycin slightly affected the cell viability. However, oligomycin deteriorated apoptosis to 40% in the condition that the viability of ESA-treated cells decreased to 70% (Figure 6c).

ESA activates protein phosphatases. The effect of ESA on enzymatic activity of a Ser/Thr phosphatase, calcineurin, was examined in the presence or absence of calmodulin. ESA activated enzymatic activity of calcineurin by two fold even in the absence of calmodulin (Figure 7a). Okadaic acid, a phosphatase inhibitor, significantly suppressed ESA-mediated apoptosis (Figure 7b). ESA may activate phosphatases including calcineurin, which resulted in dephosphorylation of RIP1.

Discussion

In this study, we describe a novel type of neuronal cell death. ESA-mediated apoptosis is regulated by AIF, ERK, RIP1 and ROS, which are key molecules of apoptosis and necroptosis. The double knockdown experiment of AIF and RIP1 suggests that they may function in the same signaling cascade. As is well known, Nec1 can inhibit TNF-α receptor-mediated necroptosis. Nec1 blocked ESA-mediated apoptosis. Interestingly, Nec1i, which is ineffective in protecting the necroptosis, also suppressed ESA-mediated apoptosis. On the other hand, RIP3 essential for necroptosis was not involved in ESA-mediated apoptosis. Caspase-8 and FADD were not changed. Together, ESA-mediated apoptosis is neither necroptosis nor RIP-dependent apoptosis triggered by TNF receptor and deletion of cIAP. One of the key events in ESA-mediated apoptosis is ROS generation in mitochondria. Like Toc, U0126 blocked ROS generation. MEK/ERK pathway may function upstream of ROS generation. Antioxidants blocked ROS generation and ESA-mediated apoptosis. Among them, Toc and BHT were effective at physiological concentrations (2 and 12.5 μg/ml, respectively), both of which are known to be diffused into intracellular organelles such as mitochondria and ER.[27,34]

The decrease in ATP levels in ESA-treated cells was a time- and a dose-dependent. Nec1 recovered the decrease in ATP; however, Nec1 did not inhibit dephosphorylation of both AIF and RIP1. ERK/1/2 and Akt are also phosphorylated upon ESA stimulation.[27] In spite of ATP depletion by ESA, these kinases are phosphorylated. This means that the dephosphorylation event is specific for AIF and RIP1. Also, the dephosphorylation is not derived from ATP depletion. ESA does not affect the intracellular GSH level, indicating that ESA does not elicit oxidative stress. It is unlikely that oxidative stress disrupts phosphatases to induce nonspecifically irreversible phosphorylation.

AIF is localized to the nucleus. Mn-SOD and COX-Vα, both of which are localized in the matrix of mitochondria, are released to the cytoplasm. After ESA stimulation, cells retained the mitochondrial membrane potential until the final stage of the cell death, although it was in part reduced. On the other hand, loss of the inner and outer membranes was observed in several percentages of mitochondria in ESA-treated cells. Disruption of both membranes can explain the release of matrix proteins.

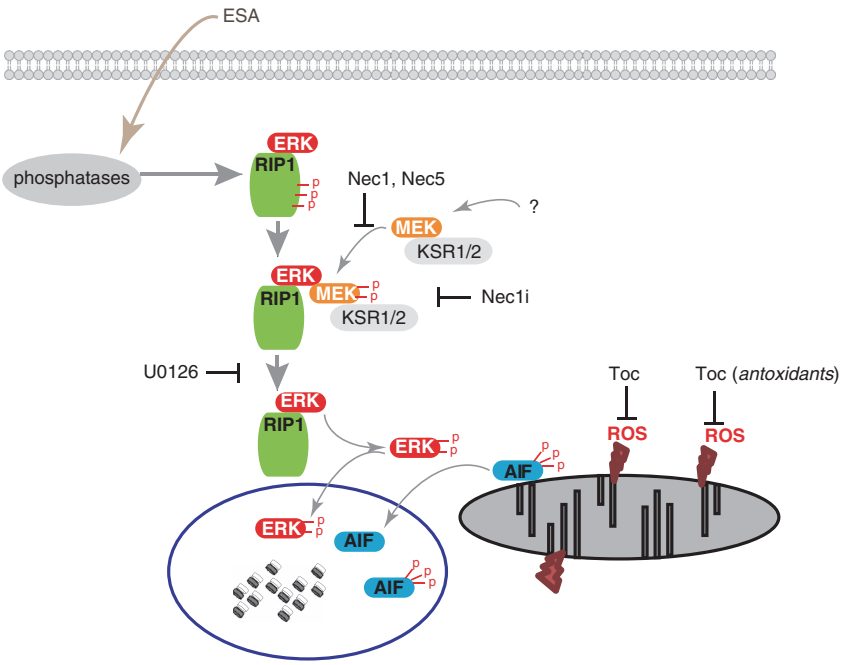

Figure 8 Proposed mechanisms of atypical RIP1-dependent cell death by ESA. (1) ESA activates phosphatases such as calcineurin, resulting in dephosphorylation of RIP1. (2) Phosphorylated MEK1/2/ activates ERK1/2 associated with RIP1. (3) AIF dephophosrylation occurs. (4) Localization of AIF and ERK1/2 in the nucleus initiates the cell death accompanied by ROS generation in mitochondria. Toc blocks the final stage of ROS production effectively, by which cells can survive.

MEK/ERK pathway appears to be involved in ESA-mediated apoptosis. ESA initiates ERK1/2 phosphorylation. RIP1 constitutively associates with ERK1/2, and transiently associates with MEK2. Nec1 and Nec5, not Nec1i, blocked phosphorylation of MEK1/2. RIP1 can mediate MEK/ERK signaling cascades in a manner different from that previously published, such as dephosphorylation. The kinase activity of RIP1 does not appear to be required for JNK activation.[22,23] The question to be answered is how ESA stimulates RIP1. Dephosphorylation of AIF and RIP1 occurs independently of ATP level in ESA-treated cells. The dephosphorylation event is likely to be upstream of RIP1. The enzymatic activity of calcineurin, a member of Ser/Thr phosphatases, is enhanced by ESA in the absence of calmodulin. Okadaic acid, a Ser/Thr phosphatase inhibitor, significantly reduces ESA-mediated apoptosis. Taken together, ESA may first acts on phosphatases to activate their enzymatic activity, resulting in dephosphorylation of RIP as well as AIF. RIP1 as well as AIF has a number of serine residues in the molecule. In RIP1, Ser14/15, Ser20 and Ser161 are related to RIP1 kinase activity. There are many other serine residues including Ser303, Ser330/331 at the C-terminus, constitutively phosphorylated. As the kinase activity of RIP1 appears not to be involved in ESA-mediated apoptosis, dephosphorylation of RIP1 may be important for ESA-mediated apoptosis rather than the phosphorylation.

MEK1/2 inhibition blocked ESA-mediated apoptosis. Together with AIF/ERK localization in the nucleus, we think that the simultaneous localization of AIF and ERK1/2 may have a significant role in ESA-mediated apoptosis. Lep-B treatment affects the cell viability more severe in $\Delta N102$-AIF-transfected cells than that in GFP-transfected cells.

Mitochondrial fission and fusion can affect apoptotic cell death. During Bax/Bak-mediated apoptosis, mitochondria are fragmented by Drp1 recruitment into mitochondria.[35–37] In contrast, mitochondrial fusion protects cells from apoptosis.[38,39] In this study, Drp1 is not involved in ESA-mediated apoptosis. A smac mimetic activates caspase-8 through the TNF-α receptor, leading to the formation of the caspase-8/FADD/RIP1 apoptotic complex IIb and cell death.[2,40] z-VAD-fmk switches from apoptosis to necrosis in some cell types such as L929 and Jurkat T cells. RIP3 determines necroptosis.[9] The phosphorylation of RIP-1 and RIP3 stabilizes their complex and regulates necroptosis.[10] Here, we show that RIP1 regulates ESA-mediated apoptosis independently of caspase-8 and FADD, which is a novel type of RIP1-dependent cell death. ESA-mediated apoptosis occurs in the caspase-8-deficient line, SH-SY5Y. Mitochondrial disruption finally resulted in cell death through ROS production.

We conclude that ESA activates phosphatases such as calcineurin followed by dephosphorylation of RIP1 as well as AIF, which results in the activation of ERK signaling pathway through MEK1/2 activation. The nuclear localization of AIF and dephosphorylation are also important in ESA-mediated apoptosis. ESA finally triggers ROS generation and the decrease in ATP in mitochondria. This leads to atypical RIP1-dependent cell death (Scheme in Figure 8).

Materials and Methods

Cell culture. PC12 (JCRB0266) cells were grown in Dulbecco's modified Eagle's medium (DMEM) supplemented with 10% horse serum and 5% fetal calf serum (FCS), penicillin and streptomycin (Life Technology, Carlsbad, CA, USA). Human neuroblastoma (SH-SY5Y) cells (American Type Culture Collection

(ATCC, Manassas, VA, USA), CRL-2266) were grown in DMEM/F-12 supplemented with 10% FCS. Mouse neuroblastoma × rat glioma hybrid (NG108-15) cells (ATCC, HB-12317) were grown in DMEM supplemented with 10% FCS. Mouse oligodendrocyte precursor FBD-102b cells were a kind gift of J. Yamauchi, National Center for Child Health and Development, originally from Y. Tomooka, Tokyo University of Science. These cells were grown in DMEM/F-12 supplemented with 10% FCS. Balb/c 3T3 (clone A31, ATCC, CCL-163) fibroblasts were grown in DMEM with 10% FCS. PC12 cells were induced to differentiate by treatment with 50 ng/ml nerve growth factor (NGF)-7S (Sigma, St. Louis, MO, USA), and were maintained at 37 °C with 5% CO_2. SH-SY5Y and NG108-15 cells were induced to differentiate by treatment with 10 μM all-*trans* retinoic acid (Sigma) and 250 μM dibutyryl cyclic AMP (Tocris, Bristol, UK), respectively. FBD-102b cells were differentiated by culturing in 0.5% FCS-containing DMEM/F-12 on polylysine-coated plates. PC12 and NG108-15 cells were differentiated on polylysine-coated plates or glass chambers. Primary neurons from the rat cortex were obtained from Lonza (R-Cx-500, Basel, Switzerland) and maintained on lysine/laminin-coated 24-well plates or 8-well chambers in Neurobasal medium with B27 supplement. The medium was changed to Neurobasal medium containing B27 minus antioxidants (B27-AO) for more than 5 days before ESA treatment on the cells for assay to avoid the effect of antioxidants in B27.

Cell viability assay. Cell viability was measured by a WST-8 assay (Cell Count Reagent SF; Nacalai, Japan). Briefly, cells were differentiated for more than 48 h, and then ESA was added to cells. After 16 h, the cell count reagent (2-(2-methoxy-4-nitrophenyl)-3-(4-nitrophenyl)-5-(2,4-disulfophenyl)-2H tetrazolium) for the WST-8 assay was added to cell cultures followed by incubation for 1–2 h. For proliferating cells, ESA was added at 16–18 h after seeding the cells. For rat cortical neurons, cells cultured in B27-AO-supplemented media were treated with ESA (20 μg/ml) for 48 or 72 h, and then the WST-8 assay was carried out. Cell viability was measured at 450 and 650 nm (as a reference) absorbance. When pre-treatment with a specific inhibitor was needed, the inhibitor was added to cell cultures at 30 min prior to ESA. ATP production and intracellular GSH were measured using CellTiter-Glo Luminescent Cell Viability Assay kit and GSH-Glo Glutathione assay kit, respectively (Promega, Madison, WI, USA).

Antibodies and chemicals. Antibodies against MEK (61B12), ERK, phospho-ERK, caspase-3 and glyceraldehyde 3-phosphate dehydrogenase (GAPDH, clone 14C10) were purchased from Cell Signaling Technology (Danvers, MA, USA). Phospho-ERK pathway sampler kit was purchased from Cell signaling Technology. ERK antibodies against AIF (E-1 and D-20), Cyt-c (7H8), Bcl-2 (C-2), Bcl-X_L (H-5), caspase-8 (D-8), ubiquitin (P4D1), FADD (H-181), Ub (P4D1) and β-actin (C-4) were purchased from Santa Cruz Biotechnology (Dallas, TX, USA). Antibodies against cIAP1 and ubiquitin (Lys63-specific) were obtained from Millipore (Billerica, MA, USA). Antibodies against MEK2 (96/MEK2), RIP1 (38/RIP) and DLP1 (also referred to as Drp1, 8/DLP1) were purchased from BD Biosciences (San Jose, CA, USA). Anti-Mn-SOD Anti-RIP3 and necrostatin-1 were obtained from Enzo Life Sciences (Farmingdale, NY, USA). Anti-LC3 was obtained from MBL. Anti-cyclophilin-A was purchased from Abcam. Antibody against complex Vα-subunit (COX Vα, clone 15H4C4) was obtained from MitoScinecne (Eugene, OR, USA). Hoechst 33342 was obtained from Life Technology. *In Situ* Cell Death Detection Kit, TMR red was used for TUNEL assay (Roche Applied Science, Burgess Hill, UK). The pan-caspase inhibitor Z-VAD-fmk and U0126 were obtained from Promega. TNF-α was obtained from PEPROTECH (Rocky Hill, NJ, USA). MitoTracker Red CM-H2Ros and MitoSOX Red were purchased from Life Technology to stain with the mitochondria. Highly pure ESA was purchased from Larodan Fine Chemicals (Malmo, Sweden). BESSo-AM was purchased from Wako Pure Chemicals (Osaka, Japan). Mdivi-1 was purchased from Sigma. ESA-Me was prepared by reacting ESA with trimethylsilyl-diazomethahne in a 10% hexane solution (TCI, Kyoto, Japan) as described elsewhere.[27] Okadaic acid, rotenone and oligomycin were purchased from Wako Pure Chemical. BHT was purchased from Nacalai (Japan). *N*-acetyl cystein (NAC), carbonyl cyanide *m*-chlorophenyl hydrazone (CCCP), leptomycin B (Lep-B), antimycin A and BSO were purchased from Sigma-Aldrich. Calcineurin enzyme activity was measured using Calcineurin Phosphatase Assay Kit (Enzo Life Sciences) according to the manufacturer's protocol. In this assay, several fatty acids were used to compare the activity, such as ESA, linolenic, linoleic, conjugated linoleic and stearic acids (all from Sigma-Aldrich). The activity of stearic acid was the same as control (DMSO). Sesamin, sesaminol and EGCG (> 99%) were purchased from Nagara Science (Gifu, Japan). Quercetin was purchased from EXTRASYNTHESE (Genay Cedex, France). A high-molecular-weight (MW) fraction of GSP (grape seed procyanidins, average MW is 3000) was prepared and obtained from Kikkoman Co Ltd. (Noda, Japan).

Immunoblotting. PC12 cells were cultured at 6×10^5 cells/dish in 10-cm poly-L-lysine-coated dishes under a differentiation condition. After 24 h, cells were cultured with NGF for another 48 h. ESA was then added to cell cultures to induce apoptosis after inhibitors, U0126 or Toc, were added when appropriate. The cells were collected after 16 h of ESA treatment. Briefly, after cells were washed with Tris-buffered saline (TBS), lysates were prepared using a Triton-based lysis buffer containing protease and phosphatase inhibitors. Neurotropic factor was included in the washing buffer to avoid other types of apoptosis caused by neurotropic factor withdrawal from differentiating cells. A mitochondrial Isolation kit (Thermo Scientific, Waltham, MA, USA) was used to prepare cytosolic and mitochondrial fractions. Phosphoproteins were purified using a PhosphoProtein Purification kit and Nanosep Ultrafiltration Column (QIAGEN, Venlo, Netherlands) according to the manufacturer's protocols. Samples were prepared from differentiated PC12 cells ($4.5–5.4 \times 10^5$ cells per 10-cm dish). Cell lysates, subcellular fractions, and purified phosphoprotein samples were resolved by SDS-polyacrylamide gel electrophoresis on 5–20% gradient gels, and then transferred onto polyvinylidene fluoride membranes (ATTO, Japan). Membranes were incubated with primary antibodies at 4 °C overnight, and then visualized with alkaline phosphatase-labeled secondary antibodies for 1 h at room temperature. Blots were visualized by an AP-conjugated substrate kit (BioRad, Hercules, CA USA). Alternatively, enhanced ECL plus (GE Healthcare, Little Chalfont, UK) was used to visualize blots after incubation of horseradish peroxidase-labeled antibodies using an LAS-4000 mini (Fujifilm, Tokyo, Japan).

Immunoprecipitation. Lysates were immunoprecipitated with appropriate antibodies, and resulting samples were probed with primary antibodies. Protein A/G-agarose was used. In addition, to reduce the influence of antibodies used in immunoprecipitation, ImmunoCruz Optima C system beads were used according to the manufacturer's protocol. Briefly, the beads (25% v/v) and 2 μg of antibody were incubated for 1.5 h at 4 °C, centrifuged at 13 000 *g* for 30 s), and then washed with PBS to form a beads- antibody complex. After preclearing with Optima C system beads, precleared lysates were incubated with the beads–antibody complex at 4 °C overnight. After washing, samples were resuspended in sample buffer for westernblot analysis.

Immunofluorescence. PC12 cells on poly-L-lysine-coated glass chamber slides were washed twice with DPBS containing NGF before the cells were fixed with 4% paraformaldehyde for 30 min, and then permeabilized with cold 0.2% Triton X-100 for 10 min. After blocking with 2% bovine serum albumin for 1 h, cells were incubated with primary antibodies. Cells were washed and incubated with Alexa 488- or TexasRed-labeled secondary antibodies and Hoechst 33342 (Life Technology) at room temperature for 1 h. After washing, cells were mounted with Prolong gold mounting media (Life Technology). Fluorescence microscopy was performed using an IX71 microscope (Olympus, Tokyo, Japan), confocal microscopes, LSM 5 Pascal (CarlZeiss, Oberkochen, Germany) and TCS-SP5 (Leica Microsystems, Solms, Germany) confocal microscopes.

Overexpression. The plasmid for Bcl-2 was constructed as described elsewhere.[27] Bcl-X_L in pcDNA 3 was a kind gift from Haruo Okado (Tokyo Metropolitan Institute for Neuroscience). Bcl-2 and Bcl-X_L were overexpressed in PC12 cells by an electroporation method (1×10^6 cells/cuvette, Amaxa Nucleofector II; Lonza) according to the manufacturer's protocol (program No. U-029). Identical numbers of transfected cells were seeded onto 35-mm dishes under the differentiation condition. At 24 h after the transfection, cells were exposed to ESA for an additional 24 h. Drp-1 was overexpressed using Lipofectamine 2000 (1×10^6 cells/ml, Life Technology). Cell viability was then measured by a WST-8 assay. For AIF overexpression, total RNA was extracted from PC12 cells using Sepasol RNA I Super (Nacalai, Japan) and cDNA was synthesized using Super Script III RT (Life Technology). Rat AIF was then cloned into the *Xho* I/*Eco*RI restriction site of the pAcGFP-N1 vector (TAKARA BIO Inc) using PCR primers (forward:5′-TCAGATCTCGAGCACCATGTTCCGGTGTGGA GGC-3′ for wild-type and 5′-GAATTCCTCGAGCACCATGCTGTCACCAGAAGAG AAA-3′ for deletion mutants of AIF lacking the first 102 amino acids (designated as Δ*N*102-AIF), reverse:5′-ACTGCAGAATTCGATCTTCATGAATGTTGAA-3′). The construct was then used to subclone the *Xho*I and *Dra*I digested fragment into the

Xho I/*Dra* I restriction site of the pCAGGS vector. Rat AIF plasmids with or without a GFP tag were constructed and confirmed by DNA sequences.

RNA Interference. Knockdowns of AIF, Drp1, RIP1, RIP3 Cyp-A by siRNA were performed in PC12 and SH-SY5Y cells. siRNAs were obtained for Drp1 (Rat 1, 5′-ACAUCUAGCAAAUUGACAGCAUGGC-3′; rat 2, 5′-UUAUGUACC AUUUCAUUUGUCACGG-3′; rat 3, 5′-UAACCUCACAAUCUCGCUGUUCUC G-3′,and human 1, 5′-AAACCUCAGGCACAAAUAAAGCAGG-3′; human 2, 5′-A UUUGAGGCAGCUGGAUGAUGUCGG-3′; human 3, 5′-UAUUAUUGUUCAUUA GCCCACAAGC-3′, Life Technology), rat AIF (rat 1, 5′-CAUAGAAGCAUGCAG CAUCUCCUGC -3′; rat 2, 5′-UGAUCAUGAUGUUCUACUCUCCUUC-3′; rat 3, 5′-AUAACUGUAAUUGACUUGACUUCCC-3′, Life Technology), rat RIP1 (5′-C UAUGAGAAUGUCAUCUGUTT -3′; rat 2, 5′-CAAGUGUAAGCCAAUCAUATT -3′, Sigma), for rat RIP3 (rat 1, 5′-CAUUAUCUGUCUCAGUACATT -3′; rat 2, 5′-C UGAGAACCUCGAGUGGGATT -3′, Sigma) and rat Cyp-A (ON-TARGET plus smart pool; Darmacon, Thermo Scientific). ON-TARGET plus siCONTROL (Darmacon, Thermo Scientific) or Negative Universal Control (Life Technology) was used as a control for nonsequence-specific effects. Transfection efficiencies were optimized using an siRNA optimization kit (Amaxa, Lonza). Transfections were performed by electroporation (Amaxa, Lonza), and identical numbers of transfected cells were seeded onto 35 mm dishes. After 24 h of incubation under the differentiation condition, cells were exposed to ESA for an additional 24 h. Cell viability was then measured using a WST-8 assay, and western blot analysis was performed to confirm protein expression.

ROS measurement. Intracellular and mitochondrial superoxides were measured using BeSSo-AM (10 μM) and MitoSOX Red (2.5 μM), respectively. Differentiated PC12 cells were incubated with BeSSo-AM or MitoSOX for 1 h or 10 min, respectively. After washing, ESA was added to cell cultures. Fluorescent intensity was measured using the MetaMorph (Meta Imaging Series ver. 7.7.7; Molecular Devices, Sunnyvale, CA, USA) software. Images from three different fields were used to quantify the intensity.

Electron microscopy. Transmission electron microscopy (TEM) was performed by Y. Ishihara (Tokai-EMA Inc., Nagoya, Japan). Briefly, cells were fixed with 2% glutaraldehyde, contrasted with OsO_4, sectioned at 70 nm thickness and then subjected to TEM analysis (JEM-1200EX, Jeol, Tokyo, Japan).

Statistical analysis. Data were expressed as the mean ± standard deviation (S.D.). The statistical significance was evaluated by one-way analysis of variance followed by the Dunnett's test to compare data from multiple groups against a common control group or Turkey's test (SigmaPlot ver.11, Chicago, IL, USA). The Student's *t*-test was used to compare data from two groups. Statistical significance (*) was determined at $P < 0.05$.

Conflict of Interest

The authors declare no conflict of interest.

Acknowledgements. We thank S. Strack (University of Iowa Carver College of Medicine) for cDNAs of rat Drp-1 and its mutants, and H. Niwa (RIKEN Center for Developmental Biology) for the pCAGGS vector. This work was supported by Grants-in-Aid for Scientific Research from the Ministry of Education, Culture, Sports, Science and Technology of Japan (2059132 to KK), and the Japan Health Sciences Foundation (KHB1201 to RT).

1. Vandenabeele P, Galluzzi L, Vanden Berghe T, Kroemer G. Molecular mechanisms of necroptosis: an ordered cellular explosion. *Nat Rev Mol Cell Biol* 2010; **11**: 700–714.
2. Wang L, Du F, Wang X. TNF-alpha induces two distinct caspase-8 activation pathways. *Cell* 2008; **133**: 693–703.
3. Micheau O, Tschopp J. Induction of TNF receptor I-mediated apoptosis via two sequential signaling complexes. *Cell* 2003; **114**: 181–190.
4. Artus C, Boujrad H, Bouharrour A, Brunelle MN, Hoos S, Yuste VJ *et al.* AIF promotes chromatinolysis and caspase-independent programmed necrosis by interacting with histone H2AX. *Embo J* 2010; **29**: 1585–1599.
5. Vandenabeele P, Declercq W, Van Herreweghe F, Vanden Berghe T. The role of the kinases RIP1 and RIP3 in TNF-induced necrosis. *Science signaling* 2010; **3**: re4.
6. Christofferson D E, Yuan J. Necroptosis as an alternative form of programmed cell death. *Curr Opin Cell Biol* 2010; **22**: 263–268.
7. Berghe T V, Vanlangenakker N, Parthoens E, Deckers W, Devos M, Festjens N *et al.* Necroptosis, necrosis and secondary necrosis converge on similar cellular disintegration features. *Cell Death Differ* 2010; **17**: 922–930.
8. Zhang D W, Shao J, Lin J, Zhang N, Lu B J, Lin S C *et al.* RIP3, an energy metabolism regulator that switches TNF-induced cell death from apoptosis to necrosis. *Science* 2009; **325**: 332–336.
9. He S, Wang L, Miao L, Wang T, Du F, Zhao L *et al.* Receptor interacting protein kinase-3 determines cellular necrotic response to TNF-alpha. *Cell* 2009; **137**: 1100–1111.
10. Cho Y S, Challa S, Moquin D, Genga R, Ray TD, Guildford M *et al.* Phosphorylation-driven assembly of the RIP1-RIP3 complex regulates programmed necrosis and virus-induced inflammation. *Cell* 2009; **137**: 1112–1123.
11. Holler N, Zaru R, Micheau O, Thome M, Attinger A, Valitutti S *et al.* Fas triggers an alternative, caspase-8-independent cell death pathway using the kinase RIP as effector molecule. *Nat Immunol* 2000; **1**: 489–495.
12. Festjens N, Vanden Berghe T, Cornelis S, Vandenabeele P. RIP1, a kinase on the crossroads of a cell's decision to live or die. *Cell Death Differ* 2007; **14**: 400–410.
13. Upton JW, Kaiser WJ, Mocarski ES. Virus inhibition of RIP3-dependent necrosis. *Cell Host & Microbe* 2010; **7**: 302–313.
14. Sun L, Wang H, Wang Z, He S, Chen S, Liao D *et al.* Mixed lineage kinase domain-like protein mediates necrosis signaling downstream of RIP3 kinase. *Cell* 2012; **148**: 213–227.
15. Wang Z, Jiang H, Chen S, Du F, Wang X. The mitochondrial phosphatase PGAM5 functions at the convergence point of multiple necrotic death pathways. *Cell* 2012; **148**: 228–243.
16. Tenev T, Bianchi K, Darding M, Broemer M, Langlais C, Wallberg F *et al.* The Ripoptosome, a signaling platform that assembles in response to genotoxic stress and loss of IAPs. *Mol Cell* 2011; **43**: 432–448.
17. Duprez L, Bertrand MJ, Vanden Berghe T, Dondelinger Y, Festjens N, Vandenabeele P. Intermediate domain of receptor-interacting protein kinase 1 (RIPK1) determines switch between necroptosis and RIPK1 kinase-dependent apoptosis. *J Biol Chem* 2012; **287**: 14863–14872.
18. Takahashi N, Duprez L, Grootjans S, Cauwels A, Nerinckx W, DuHadaway JB *et al.* Necrostatin-1 analogues: critical issues on the specificity, activity and in vivo use in experimental disease models. *Cell Death Dis* 2012; **3**: e437.
19. Vandenabeele P, Grootjans S, Callewaert N, Takahashi N. Necrostatin-1 blocks both RIPK1 and IDO: consequences for the study of cell death in experimental disease models. *Cell Death Differ* 2013; **20**: 185–187.
20. Degterev A, Maki JL, Yuan J. Activity and specificity of necrostatin-1, small-molecule inhibitor of RIP1 kinase. *Cell Death Differ* 2013; **20**: 366.
21. Lee TH, Huang Q, Oikemus S, Shank J, Ventura JJ, Cusson N *et al.* The death domain kinase RIP1 is essential for tumor necrosis factor alpha signaling to p38 mitogen-activated protein kinase. *Mol Cell Biol* 2003; **23**: 8377–8385.
22. Ting AT, Pimentel-Muinos FX, Seed B. RIP mediates tumor necrosis factor receptor 1 activation of NF-kappaB but not Fas/APO-1-initiated apoptosis. *Embo J* 1996; **15**: 6189–6196.
23. Yuasa T, Ohno S, Kehrl JH, Kyriakis JM. Tumor necrosis factor signaling to stress-activated protein kinase (SAPK)/Jun NH2-terminal kinase (JNK) and p38. Germinal center kinase couples TRAF2 to mitogen-activated protein kinase/ERK kinase kinase 1 and SAPK while receptor interacting protein associates with a mitogen-activated protein kinase kinase kinase upstream of MKK6 and p38. *J Biol Chem* 1998; **273**: 22681–22692.
24. Kelliher MA, Grimm S, Ishida Y, Kuo F, Stanger BZ, Leder P. The death domain kinase RIP mediates the TNF-induced NF-kappaB signal. *Immunity* 1998; **8**: 297–303.
25. Yanai I, Benjamin H, Shmoish M, Chalifa-Caspi V, Shklar M, Ophir R *et al.* Genome-wide midrange transcription profiles reveal expression level relationships in human tissue specification. *Bioinformatics* 2005; **21**: 650–659.
26. Selman C, Kerrison ND, Cooray A, Piper MD, Lingard SJ, Barton RH *et al.* Coordinated multitissue transcriptional and plasma metabonomic profiles following acute caloric restriction in mice. *Physiological Genomics* 2006; **27**: 187–200.
27. Kondo K, Obitsu S, Ohta S, Matsunami K, Otsuka H, Teshima R. Poly(ADP-ribose) polymerase (PARP)-1-independent apoptosis-inducing factor (AIF) release and cell death are induced by eleostearic acid and blocked by alpha-tocopherol and MEK inhibition. *J Biol Chem* 2010; **285**: 13079–13091.
28. Hasegawa T, Ishibashi M, Takata T, Takano F, Ohta T. Cytotoxic fatty acid from Pleurocybella porrigens. *Chem Pharm Bull* 2007; **55**: 1748–1749.
29. Wakimoto T, Asakawa T, Akahoshi S, Suzuki T, Nagai K, Kawagishi H *et al.* Proof of the existence of an unstable amino acid: pleurocybellaziridine in *Pleurocybella porrigens*. *Angew Chem* 2011; **50**: 1168–1170.
30. Kawaguchi T, Suzuki T, Kobayashi Y, Kodani S, Hirai H, Nagai K *et al.* Unusual amino acid derivatives from the mushroom *Pleurocybella porrigens*. *Tetrahedron* 2010; **66**: 504–507.
31. Amakura Y, Kondo K, Akiyama H, Ito H, Hatano T, Yoshida T *et al.* Characteristic long-chain fatty acid of Pleurocybella porrigens. *Shokuhin Eiseigaku zasshi* 2006; **47**: 178–181.
32. Amakura Y, Kondo K, Akiyama H, Ito H, Hatano T, Yoshida T *et al.* Conjugated ketonic fatty acids from Pleurocybella porrigens. *Chem Pharm Bull* 2006; **54**: 1213–1215.
33. Zhu C, Wang X, Deinum J, Huang Z, Gao J, Modjtahedi N *et al.* Cyclophilin A participates in the nuclear translocation of apoptosis-inducing factor in neurons after cerebral hypoxia-ischemia. *J Exp Med* 2007; **204**: 1741–1748.

34. Akasaka R, Teshima R, Kitajima S, Momma J, Inoue T, Kurokawa Y *et al.* Effects of hydroquinone-type and phenolic antioxidants on calcium signals and degranulation of RBL-2H3 cells. *Biochem Pharmacol* 1996; **51**: 1513–1519.
35. Martinou JC, Youle RJ. Mitochondria in apoptosis: Bcl-2 family members and mitochondrial dynamics. *Dev Cell* 2011; **21**: 92–101.
36. Frank S, Gaume B, Bergmann-Leitner ES, Leitner WW, Robert EG, Catez F *et al.* The role of dynamin-related protein 1, a mediator of mitochondrial fission, in apoptosis. *Dev Cell* 2001; **1**: 515–525.
37. Wasiak S, Zunino R, McBride HM. Bax/Bak promote sumoylation of DRP1 and its stable association with mitochondria during apoptotic cell death. *J Cell Biol* 2007; **177**: 439–450.
38. Lee YJ, Jeong SY, Karbowski M, Smith CL, Youle RJ. Roles of the mammalian mitochondrial fission and fusion mediators Fis1, Drp1, and Opa1 in apoptosis. *Mol Biol Cell* 2004; **15**: 5001–5011.
39. Sugioka R, Shimizu S, Tsujimoto Y. Fzo1, a protein involved in mitochondrial fusion, inhibits apoptosis. *J Biol Chem* 2004; **279**: 52726–52734.
40. Li L, Thomas RM, Suzuki H, De Brabander JK, Wang X, Harran PG. A small molecule Smac mimic potentiates TRAIL- and TNFalpha-mediated cell death. *Science* 2004; **305**: 1471–1474.

Supplementary Information accompanies this paper on Cell Death and Disease website (http://www.nature.com/cddis)